

# Journal of Materials Chemistry A

Materials for energy and sustainability

Accepted Manuscript

This article can be cited before page numbers have been issued, to do this please use: G. Liu, H. Cui, S. Wang, L. Zhang and C. Su, *J. Mater. Chem. A*, 2020, DOI: 10.1039/D0TA02033H.



This is an Accepted Manuscript, which has been through the Royal Society of Chemistry peer review process and has been accepted for publication.

Accepted Manuscripts are published online shortly after acceptance, before technical editing, formatting and proof reading. Using this free service, authors can make their results available to the community, in citable form, before we publish the edited article. We will replace this Accepted Manuscript with the edited and formatted Advance Article as soon as it is available.

You can find more information about Accepted Manuscripts in the [Information for Authors](#).

Please note that technical editing may introduce minor changes to the text and/or graphics, which may alter content. The journal's standard [Terms & Conditions](#) and the [Ethical guidelines](#) still apply. In no event shall the Royal Society of Chemistry be held responsible for any errors or omissions in this Accepted Manuscript or any consequences arising from the use of any information it contains.

## ARTICLE

# A series of highly stable porphyrinic metal-organic frameworks based on iron-oxo chain cluster: design, synthesis and biomimetic catalysis

Received 00th January 20xx,  
Accepted 00th January 20xx

DOI: 10.1039/x0xx00000x

Gang Liu, Hao Cui, Sujuan Wang, Li Zhang\* and Cheng-Yong Su\*

Iron-based porphyrinic metal-organic frameworks (PMOFs) are desirable for biomimetic applications, due to the low toxicity and high abundance of Fe as well as the rich biomimetic functions of metalloporphyrins. Besides, the uniform dispersion of porphyrin centers in PMOFs can effectively prevent them from self-dimerization. Nevertheless, it remains a big challenge to synthesize iron-based PMOFs. In this study, a series of Fe-oxo chain-based PMOFs incorporating different metals in porphyrinic centers (namely M-PMOF-3(Fe), M = Fe, Co, Ni, Cu) are synthesized directly from the reaction of metalloporphyrin and iron salts with an improved modulating strategy using a pair of monocarboxylic acids and water as the three-component modulator. The prepared materials of M-PMOF-3(Fe) possess high stability to resist a broad pH range (0-11) and even 2 M HCl in aqueous solutions for 2 days, and their frameworks can be maintained up to 350 °C. Catalytic tests show that M-PMOF-3(Fe) are effective for the aerobic oxidation of C-H bonds using the oxygen from the air as the oxidant.

## 1. Introduction

Metalloporphyrins exist widely in biological systems such as cytochrome, peroxidase, isomerase, dehalogenase and transferase, and they can initiate a range of fundamentally and practically important chemical transformations, including epoxidation of olefins, hydroxylation of C-H bonds, and oxidation of amines, sulfides, alcohols and aldehydes, even for unreactive substrates hydrocarbons under mild conditions.<sup>1-3</sup> Despite the well-demonstrated advantages, porphyrin molecules are prone to dimerization and self-oxidation deactivation in homogeneous catalytic system. In order to solve this problem, a series of immobilization methods of porphyrins have been developed, such as coating or immobilization of porphyrin molecules on molecular sieves, carbon materials, silica, etc.<sup>4-7</sup> As an alternative strategy, porphyrin compounds have been encapsulated in the cavities of metal-organic frameworks (MOFs) or behave as the organic linkers of MOFs.<sup>8-15</sup> The resultant porphyrinic metal-organic frameworks (PMOFs) display several advantages: 1) the uniform dispersion of porphyrin centers effectively prevents it from self-dimerization; 2) the porosity of MOFs makes each porphyrin unit available for incoming substrates and

accelerates the leaving of the products; 3) the heterogeneous nature of MOF endows the porphyrin-based catalysts with recyclability.<sup>16-22</sup>

Nevertheless, the ideal biomimetic performances of PMOFs are greatly limited by their stability, especially regarding to hydrolysis. Conceptually, strong coordination bonds between metal ions and ligands can assist in the formation of stable MOFs.<sup>23</sup> Based on this strategy, some stable PMOFs have been successfully prepared by employing the combination of either high valence metal ions (e.g. Ti<sup>4+</sup>, Zr<sup>4+</sup>, Hf<sup>4+</sup>, Al<sup>3+</sup>, In<sup>3+</sup> and Fe<sup>3+</sup>) with carboxylates<sup>24-33</sup> or low valence metal ions with nitrogen-containing ligands.<sup>34,35</sup> Among them, Fe<sup>3+</sup>-based PMOFs are the best adequate for biomimetic applications due to the low toxicity in biology and high abundance in Earth, but they remain difficult to synthesize.<sup>33,36,37</sup> The few reported Fe-based PMOFs are synthesized with two kinds of methods. The one is to employ preassembled Fe-oxo clusters to react with porphyrin ligands.<sup>38</sup> A series of Fe-based PMOFs named after PCN-600 have been prepared through the self-assembly of preassembled [Fe<sub>3</sub>O(OOCCH<sub>3</sub>)<sub>6</sub>] clusters and metalloporphyrins.<sup>33</sup> Due to the mesoporosity of PCN-600 with a diameter of 3.1 nm, direct activation of PCN-600 is unsuccessful. The activation needs to be carried out under supercritical carbon dioxide, after applying a dilute acid solution for pre-activation treatments. The other one is to use an either inorganic or organic base to deprotonate the carboxylic acid groups and thus facilitate the coordination of the iron ion to the porphyrin.<sup>36,37</sup> During the crystal growth, the organic bases such as 4,4'-bipyridine and pyrazine can not only deprotonate the carboxylic acid but also coordinate to the metal centers in the porphyrin ring, the latter of which makes

MOE Laboratory of Bioinorganic and Synthetic Chemistry, Lehn Institute of Functional Materials, School of Chemistry, Sun Yat-Sen University, Guangzhou 510275, China. E-mail: zhli99@mail.sysu.edu.cn; cescy@mail.sysu.edu.cn.

†Electronic Supplementary Information (ESI) available: Synthesis of metalloporphyrin ligands and porphyrinic metal-organic frameworks (PMOFs), crystal structure data, physical characterizations, stability study and catalytic performances of PMOFs. CCDC number 1892975 and 1983557. See DOI: 10.1039/x0xx00000x

the metalloporphyrin inaccessible to the incoming substrates for the further transformations.

In this work, we employ an improved modulating synthetic strategy<sup>39</sup> using a pair of monocarboxylic acids and water as the three-component modulator, and facily prepare a series of highly stable Fe-oxo chain-based porphyrinic MOFs (namely M-PMOF-3(Fe), M = Fe, Co, Ni, Cu) (Figure 1). The three-component modulator can effectively control crystal nucleation and growth.<sup>40-42</sup> The synthesis process is carried out in one-pot, and the obtained crystals display high crystallinity and purity. The frameworks of M-PMOF-3(Fe) with the *fry*-topology are composed of metalloporphyrin linkers and [Fe(OH)O<sub>4</sub>]<sub>n</sub> chains, which possess high stability, survive in a broad pH range (0-11) and even in 2 M HCl for 2 days, and can be maintained up to 350 °C. Biomimetic applications of M-PMOF-3(Fe) towards the oxidation of C-H bonds in air have been carried out thereafter.

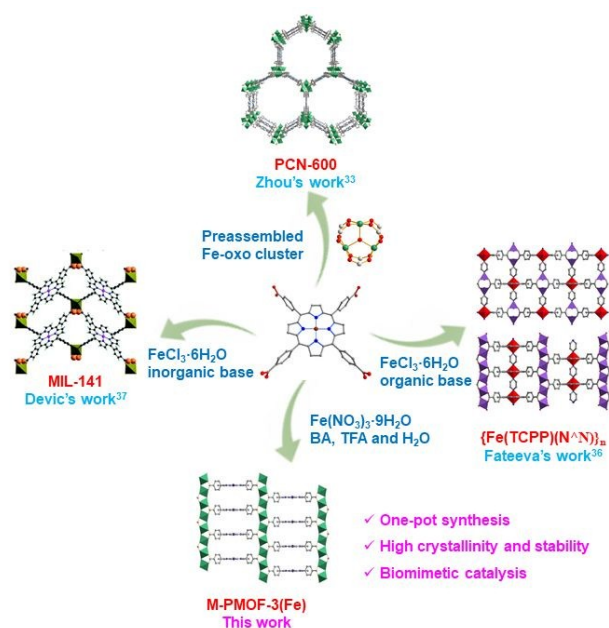


**Figure 1.** The syntheses of Fe-based porphyrinic metal-organic frameworks in previous reports and this work (M = Fe, Co, Ni, Cu). BA and TFA represent benzoic acid and trifluoroacetic acid, respectively).

## 2. Experimental Section

### 2.1 General

All chemicals used in this paper are purchased from commercial sources without further treatment. The synthesis of metalloporphyrin ligands is discussed in the Supporting Information. The single crystal X-ray diffraction data are collected using an Agilent Technologies SuperNova X-ray diffractometer system equipped with Cu-K $\alpha$  radiation (1.54178 Å). Powder X-ray diffraction (PXRD) patterns are measured on a Japan Rigaku Miniflex 600. Nitrogen adsorption-desorption isotherms are measured using a Micromeritics ASAP 2020 system at 77 K. Before the examinations, the as-synthesized samples are washed with DMF for five times, soaked in DMF

and acetone sequentially for 12 h, and then activated under vacuum at 150 °C for 12 h. Energy dispersive X-ray spectroscopy (EDS) is recorded on a JSM-6330F field emission scanning electron microscope combined with EDS. X-ray photoelectron spectroscopy (XPS) is performed on a ULVAC PHI Quantera microprobe. GC-MS data are recorded on an Agilent 7890-5975C. Thermogravimetric (TG) analysis is carried out on a Netzsch STA 449 F3 system from 30°C to 900 °C at a rate of 5 °C min<sup>-1</sup>. GC-MS data are recorded on an Agilent 7890-5975C.

### 2.2 Synthesis of M-PMOF-3(Fe)

The synthesis procedure of M-PMOF-3(Fe) (M = Fe, Co, Ni, Cu) is using Fe-PMOF-3(Fe) as a typical example: A mixture of [5,10,15,20-tetrakis(4-methoxycarbonylphenyl)porphyrinato] Fe(III) chloride that is named after Fe-TCPP (8 mg, 9.45  $\mu$ mol), Fe(NO<sub>3</sub>)<sub>3</sub>·9H<sub>2</sub>O (9 mg, 22.3  $\mu$ mol), benzoic acid (BA, 400 mg, 3.28 mmol), trifluoroacetic acid (TFA, 270  $\mu$ L, 3.64 mmol) and H<sub>2</sub>O (20  $\mu$ L, 1.11 mmol) is ultrasonically dissolved in *N,N*-dimethylacetamide (DMAC, 2 mL) in a 15 mL Teflon-lined autoclave. The autoclave is afterwards placed in a programmable oven (DHG-9145A, Keelrein instrument co. Ltd, Shanghai, China) at 160 °C for 12 h with a heating rate of 1.5 °C/min and a cooling rate of 0.38 °C/min. After being cooled down to room temperature, the dark red crystals of Fe-PMOF-3(Fe) are obtained by filtration, and washed with DMF for five times and with acetone for three times.

Anal. Calcd. for Fe-PMOF-3(Fe)·7BA·3TFA·DMF·5H<sub>2</sub>O: C, 53.41; H, 3.61; N, 2.94 Found: C, 53.23; H, 5.32; N, 2.37. FTIR (cm<sup>-1</sup>, ATR): 3402 (w), 2570 (w), 1607 (w), 1514 (m), 1410 (s), 1180 (m), 995 (m), 773 (m), 711 (m), 543 (m), 509 (m), 439 (m).

Anal. Calcd. for Co-PMOF-3(Fe)·5BA·2.3TFA·0.2DMF·4H<sub>2</sub>O: C, 54.38; H, 3.38; N, 3.02. Found: C, 54.31; H, 6.24; N, 2.66. FTIR (cm<sup>-1</sup>, ATR): 3390 (w), 1610 (w), 1578 (w), 1508 (m), 1411 (s), 1350 (m), 999 (m), 774 (m), 713 (m), 554 (w), 512 (m), 459 (m).

Anal. Calcd. for Ni-PMOF-3(Fe)·5BA·2.1TFA·4H<sub>2</sub>O: C, 54.82; H, 3.36; N, 2.93. Found: C, 54.38; H, 5.74; N, 2.43. FTIR (cm<sup>-1</sup>, ATR): 3431 (m), 2928 (w), 2350 (w), 1514 (s), 1414 (s), 1182 (w), 1001 (m), 773 (m), 712 (m), 556 (m), 516 (m), 463 (m).

Anal. Calcd. for Cu-PMOF-3(Fe)·1.8TFA·0.02DMF·3H<sub>2</sub>O: C, 55.83; H, 3.33; N, 3.02. Found: C, 55.55; H, 5.84; N, 2.57. FTIR (cm<sup>-1</sup>, ATR): 3045 (w), 2928 (w), 1517 (s), 1411 (s), 1345 (s), 1182 (m), 998 (m), 773 (m), 713 (m), 605 (w), 550 (m), 516 (m), 447 (m).

### 2.3 Typical procedure for catalytic oxidation of hydrocarbons

In a typical reaction, an acetonitrile (2 mL) solution of Cu-PMOF-3(Fe) (4 mg, 0.004 mmol) is placed into a round bottom flask (10 mL) that is equipped with a reflux condenser, and then stirred for 24 h at room temperature. Afterwards, *N*-hydroxyphthalimide (NHPI, 6 mg, 0.037 mmol) and ethylbenzene (21.2 mg, 0.2 mmol) are added to the flask. The reaction mixture is stirred at 60 °C in air for 24 h, which is then analyzed by GC-MS. The yield (82%) of the product acetophenone is determined by GC-MS.

After the reaction, Cu-PMOF-3(Fe) is separated by centrifugation, washed with acetonitrile for 3 times and then soaked in acetonitrile for 12 h. After that, Cu-PMOF-3(Fe) is

separated by centrifugation, and collected for the recycling experiments.

### 3. Results and Discussion

#### 3.1 Synthesis

Modulated synthesis has been reported to be an effective method for the synthesis of highly crystalline MOFs, especially the carboxylate-based MOFs.<sup>43-47</sup> The monocarboxylic acid as the modulator is added to the self-assembly system to compete with the organic linker, and then control crystal nucleation and growth. In the improved modulating synthesis, a trace amount of water is added to promote the hydrolysis of metal salts and accelerate the crystal nucleation. Nevertheless, modulated synthesis hasn't been successfully applied to the synthesis of Fe-based PMOFs.

Through trials and errors, single crystals couldn't be obtained by using a single monocarboxylic acid (e.g. benzoic acid (BA), trifluoroacetic acid (TFA) or acetic acid) as the modulator yet (Figures S1 and S2). To our delight, by introducing BA, TFA and H<sub>2</sub>O as the three-component modulator, the desired crystals of the Fe-based PMOFs (namely M-PMOF-3(Fe), M = Fe, Co, Ni, Cu) are obtained from the self-assembly of metalloporphyrin and Fe(NO<sub>3</sub>)<sub>3</sub>·9H<sub>2</sub>O (Figure 1). It is noted that the use of FeCl<sub>3</sub>·xH<sub>2</sub>O as the iron salt can't give rise to any crystals in this work, although this iron salt has been usually used for the synthesis of Fe-based MOFs.<sup>36,37,48,49</sup>

The effect of the amounts of BA and TFA on the crystal growth has been studied. When other reagents except BA are fixed (e.g. with the molar ratio of metalloporphyrin, Fe(NO<sub>3</sub>)<sub>3</sub>·9H<sub>2</sub>O and TFA being 3.63 : 6.11 : 1000), the crystal sizes increase with the amounts of BA increasing from 0 to 1.5 times of TFA. The crystals become wider horizontally and shorter longitudinally, and finally approximately rectangular (Figure S3). On the other hand, with the fixed amounts of metalloporphyrin, Fe(NO<sub>3</sub>)<sub>3</sub>·9H<sub>2</sub>O and BA with the molar ratio of 3.60 : 6.04 : 1000, the amount of TFA also takes an important role on the crystal growth (Figure S4). When the amount of TFA increases from 0.6 to 1.4 times of BA, the crystal sizes increase gradually and their morphologies change from spindle, cubic rod to octahedron.

The effect of the amount of water on the crystal growth is further investigated (Figure S5). In the absence of water, a rod-like crystal with uncertain structure is yielded. Meanwhile, the increase of the water amount leads to a decrease of the crystal size.

In short, the crystal nucleation and growth can be finely tuned by the three-component modulator, and highly crystalline M-PMOF-3(Fe) can be prepared by the improved modulating synthesis.

#### 3.2 Structure

Single-crystal X-ray diffraction analyses disclose that the M-PMOF-3(Fe) series are isostructural and crystallize in the orthorhombic system with the space group of *Cmmm* (Table S1). Ni-PMOF-3(Fe) is herein taken as an example to illustrate

the structure of the M-PMOF-3(Fe). Ni-PMOF-3(Fe) possesses a three-dimensional reticular structure with a *fw* topology, which is composed of Ni<sup>II</sup>-TCPP (TCPP = mesotetrakis(4-carboxyphenyl) porphyrin) linkers and Fe-oxo chains (Figure 2). Each porphyrin ligand connects four Fe-oxo chains via carboxylate groups to construct the 3D network, featuring 1D channel with the size of 13.6 × 7.2 Å<sup>2</sup> running through the *a* axis (Figure 2a). The porphyrin rings in Ni-PMOF-3(Fe) are arranged in parallel, and the distance of the adjacent porphyrin rings is 6.8 Å (Figure 2b). The Fe<sup>3+</sup> ions in the Fe-oxo chain are octahedrally coordinated by six oxygen atoms, and four of these oxygen atoms in the equatorial plane are from carboxylate groups of four different porphyrin linkers and the remaining two oxygen atoms in the axial are from two μ<sub>2</sub>-OH groups. In this way, these oxygen atoms bridge adjacent Fe(III) ions to give rise to [Fe(OH)O<sub>4</sub>]<sub>n</sub> chain (Figure 2c). PLATON calculations indicate that Ni-PMOF-3(Fe) display an effective pore volume of 57.9%. The well-defined PXRD patterns of the as-synthesized samples are consistent with the simulated pattern, indicative of the high phase purity and crystallinity of M-PMOF-3(Fe) (Figure S6).

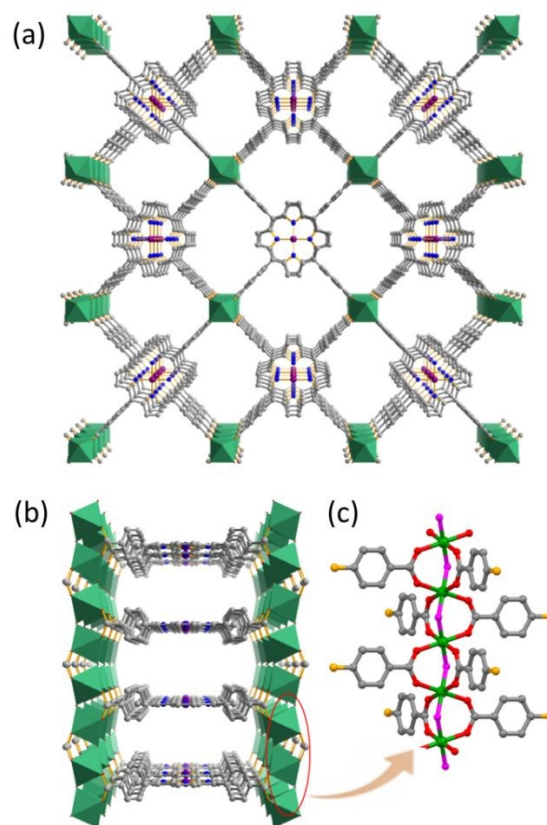


**Figure 2.** Views of the 3D network of Ni-PMOF-3(Fe) along the *a* (a) and *c* axes (b) (Ni<sup>2+</sup> ion, violet; Fe<sup>3+</sup> ion, green; N atom, blue; O atom, red). The structure of [Fe(OH)O<sub>4</sub>]<sub>n</sub> chain is shown in (c), in which the oxygen atom from μ<sub>2</sub>-OH is marked with magenta for easy identification and the porphyrin ring is represented by an orange ball. The hydrogen atoms are omitted for clarity.

The surface area and porous structure of M-PMOF-3(Fe) series are evaluated by N<sub>2</sub> adsorption-desorption isotherms at 77 K (Figure 3). They display type I isotherms, indicative of the microporosity of the structure. The Brunauer–Emmett–Teller (BET) surface areas of M-PMOF-3(Fe) (M = Fe<sup>3+</sup>, Co<sup>2+</sup>, Ni<sup>2+</sup> and Cu<sup>2+</sup>) are calculated to be 1241, 1318, 1237 and 1458 m<sup>2</sup>/g, respectively (Figures S7-10). According to the Density Functional Theory (DFT) calculations, the pore sizes of M-PMOF-3(Fe) are in the range of 7.4-7.8 Å (Table S2), which are consistent with the single-crystal analysis (7.8 Å).

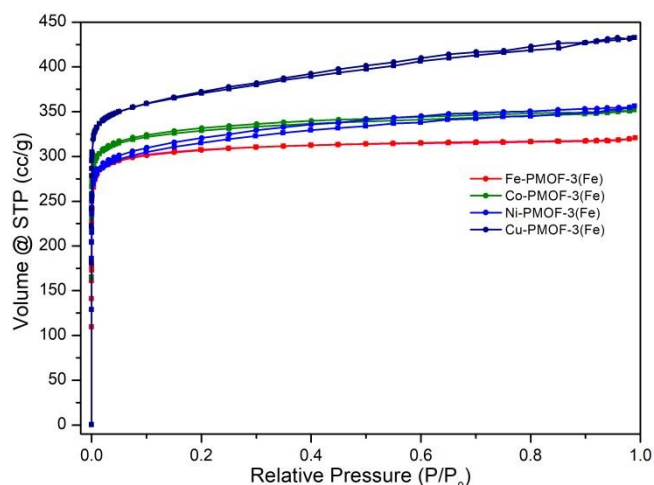


**Figure 3.** N<sub>2</sub> adsorption-desorption isotherm of M-PMOF-3(Fe).

### 3.3 Characterizations and Stability

Energy dispersive X-ray spectroscopy (EDS) discloses that C, N, O, and Fe elements exist in the M-PMOF-3(Fe) series (Figures S11-14 and Tables S3-6). In addition, Co, Ni and Cu elements occur in Co-PMOF-3(Fe), Ni-PMOF-3(Fe) and Cu-PMOF-3(Fe), respectively. The exact contents of metallic elements in M-PMOF-3(Fe) are determined by inductively coupled plasma optical emission spectroscopy (ICP-OES), which are almost close to the theoretical values (Table S7). High-resolution X-ray photoelectron spectroscopy (XPS) of M-PMOF-3(Fe) indicate that the metal elements in the metalloporphyrin are Fe<sup>3+</sup> (Fe 2p<sub>3/2</sub>, 712 eV; Fe 2p<sub>1/2</sub>, 725.7 eV), Co<sup>2+</sup> (Co 2p<sub>3/2</sub>, 780.3 eV; Co 2p<sub>1/2</sub>, 795.7 eV), Ni<sup>2+</sup> (Ni 2p<sub>3/2</sub>, 854.8 eV; Ni 2p<sub>1/2</sub>, 872.1 eV) and Cu<sup>2+</sup> (Cu 2p<sub>3/2</sub>, 934.5 eV; Cu 2p<sub>1/2</sub>, 954.4 eV), respectively, and the Fe ion in Fe-oxo chain ([Fe(OH)O<sub>4</sub>]<sub>n</sub>) is +3 (Figures S15-18 and Tables S8-11).<sup>50-53</sup>

High structural stability, especially regarding to hydrolysis, is critical for the biomimetic application of the prepared materials. After the M-PMOF-3(Fe) series are soaked in aqueous solutions with a pH range of 0-12 for 48 h, the supernatant is almost colorless in the solution of pH 0-11, but turns to dark red in the solution of pH 12. M-PMOF-3(Fe) can resist in 2 M HCl, although the supernatant is of a slight yellow color. The PXRD patterns of the recycled M-PMOF-3(Fe) samples after the above stability tests in the aqueous solutions with the pH range of 0-11 keep unchanged relative to the as-synthesized samples, indicative of their high resistance towards a broad pH range (Figures 4a and S19-21). Even under

an ultra-harsh condition (e.g. 2 M HCl), the PXRD patterns of Ni-PMOF-3(Fe) and Cu-PMOF-3(Fe) are almost unchanged, whereas those of Fe-PMOF-3(Fe) become very weak. For comparison, Al-PMOF<sup>31</sup> and USTC-8<sup>32</sup>, which are based on Al-oxo and In-oxo chains, respectively, are isomorphous to M-PMOF-3(Fe), and are reported to be stable in a pH range of 5-8 and 2-11, respectively.

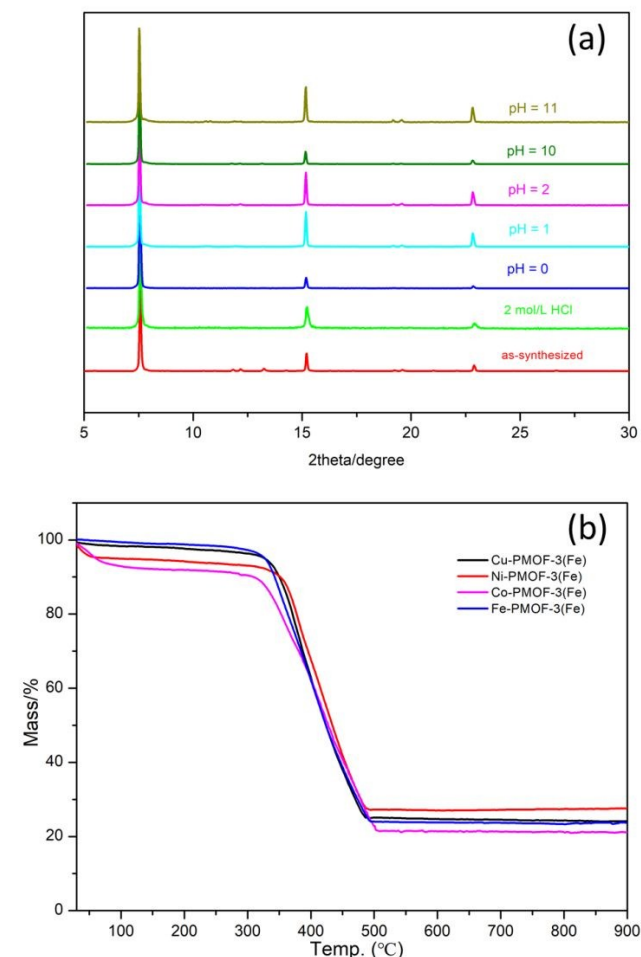


**Figure 4.** Stability test of Cu-PMOF-3(Fe) in aqueous solutions with the pH range of 0-12 and 2 M HCl for 48 h (a) and TG curves of M-PMOF-3(Fe).

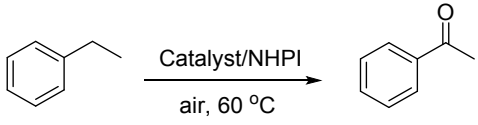
Besides, after the fresh crystals of M-PMOF-3(Fe) are immersed in a wide range of organic solvents, such as dichloromethane (DCM), ethyl acetate (EA), diethyl ether (Et<sub>2</sub>O), acetonitrile (MeCN), tetrahydrofuran (THF), methanol (MeOH) and toluene (PhCH<sub>3</sub>) for 7 days, the PXRD patterns of the recycled samples retain the prominent peak profiles (Figure S22-24). Thermogravimetric (TG) analyses further demonstrate that the frameworks of M-PMOF-3(Fe) can be maintained up to 350 °C, indicative of a relatively high thermal stability (Figure 4b).

### 3.4 Catalysis

As for an oxidation reaction, oxygen (O<sub>2</sub>), especially from the air, is obviously the most ideal oxidant, and then it is of high interests to develop catalytic oxidation systems that use O<sub>2</sub>

from the air as the oxidants. Inspired by nature, biomimetic catalytic oxidation systems have been developed by simulating cytochrome P450 enzymes to realize the activation of O<sub>2</sub> under mild conditions and further oxidation of the inert C-H bond of hydrocarbons.<sup>54</sup> Considering that the M-PMOF-3(Fe) series contain highly dispersed porphyrin sites and are highly stable, they are applied for biomimetic aerobic oxidation of hydrocarbons in air.

**Table 1. Aerobic oxidation of ethylbenzene<sup>a</sup>**



Entry	Catalyst	Yield (%)	Ketone Selectivity (%)
1	Fe-PMOF-3(Fe)	61	97
2	Co-PMOF-3(Fe)	26	88
3	Ni-PMOF-3(Fe)	8	79
4	Cu-PMOF-3(Fe)	82 (93) <sup>b</sup>	98 (98) <sup>b</sup>
5	No catalyst	13	79

<sup>a</sup>Reaction conditions: A mixture of ethylbenzene (21.2 mg, 0.2 mmol), NHPI (6 mg, 0.037 mmol) and catalyst (0.004 mmol) is stirred in acetonitrile (2 mL) at 60°C under atmospheric pressure for 24 h. The yield is determined by GC-MS. <sup>b</sup>The reaction time is extended to 35 h.

The aerobic oxidation of ethylbenzene in air is used as a model reaction to study the catalytic performances of M-PMOF-3(Fe) combined with *N*-hydroxyphthalimide (NHPI) as the auxiliary catalyst (Table 1). Among all of the tested catalysts, Fe-PMOF-3(Fe) and Cu-PMOF-3(Fe) are much more efficient and produce the oxidized product acetophenone in 61 and 82% yields in 24 h, respectively, and the ketone/alcohol selectivity is up to 98:2 (entries 1 and 4). With the extension of the reaction time, the yield of acetophenone is improved to 93% in 35 h. It is reported that metalloporphyrin complexes based on Fe, Co and Cu are desirable catalysts for the oxidation reactions because they can form high-valent oxo complexes with relatively high stability, which are thought to be the intermediates.<sup>3</sup> However, Co-PMOF-3(Fe) doesn't display as high performances as Fe-PMOF-3(Fe) and Cu-PMOF-3(Fe) in this work. The reason for the poor reactivity of Co-PMOF-3(Fe) with only 26% yield (entry 2) is unclear yet. The reaction in the presence of Ni-PMOF-3(Fe) is even worse than the one using NHPI alone (entries 3 and 5). In Ni-PMOF-3(Fe), Ni<sup>2+</sup>-porphyrin is square planar geometry and with d<sup>8</sup> configuration. The energy of the empty d<sub>x<sub>2</sub>-y<sub>2</sub></sub> orbital of the Ni<sup>2+</sup> ion is too high to accept electrons from O<sub>2</sub>, and thus it is difficult for the reaction to occur between Ni<sup>2+</sup>-porphyrin and O<sub>2</sub>.

On the basis of these results, Cu-PMOF-3(Fe) is selected for the following study. The advantages of Cu-PMOF-3(Fe) prior to the corresponding molecular catalyst Cu-TCPP are firstly studied. The turn-over numbers (TON) in the presence of 0.1 mol% of Cu-PMOF-3(Fe) and Cu-TCPP are 330 and 180,

respectively (Table S12). The catalytic performance of Cu-PMOF-3(Fe) is further investigated in the solvent-free system, and the conversion of ethylbenzene to acetophenone is 9% in the presence of 0.025 mol% of the catalyst in 7 days (Table S13). Moreover, the heterogeneous nature of Cu-PMOF-3(Fe) is then studied, disclosing that Cu-PMOF-3(Fe) can be easily recovered by centrifugation and maintain its high catalytic activity after 11 continuous runs (Figure 5). After catalytic reactions, the PXRD patterns of the recovered catalysts are mainly remained (Figure S25). These results disclose of the high stability of Cu-PMOF-3(Fe).

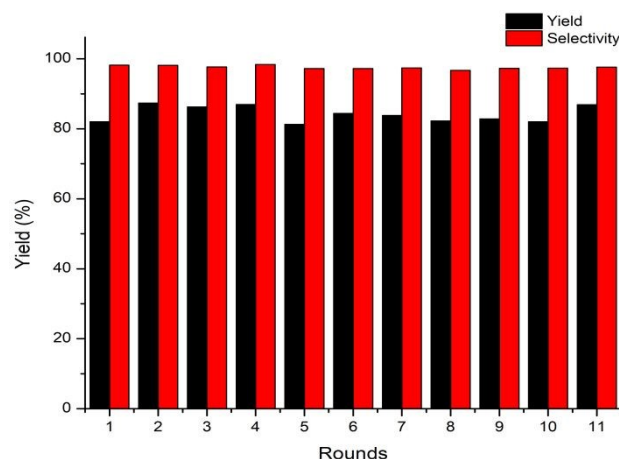


**Figure 5.** Recycling experiments of the catalytic oxidation of ethylbenzene.

Finally, other hydrocarbons are also examined in the Cu-PMOF-3(Fe)-catalyzed oxidation reactions (Table S14). The oxidative conversions of tetralin and (methoxymethyl)benzene to the corresponding ketones are 99 and 96%, respectively. For comparison, 9*H*-fluorene is less efficient and the conversion is 58%. The C-H bond dissociation energies for tetralin, (methoxymethyl)benzene and 9*H*-fluorene are 82.9, 85.8 and 80.1 kcal/mol, respectively.<sup>55,56</sup> On the basis of these data, 9*H*-fluorene should display higher efficiency than the other two due to the relatively weaker C-H bond, but however this conclusion is inconsistent with the experimental findings. On the other hand, if the catalytic reactions were carried out in the inner cavities of Cu-PMOF-Fe (13.6 × 7.2 Å<sup>2</sup>), the substrate sizes should also play an important role on the reaction efficiency. The molecular sizes of tetralin, (methoxymethyl)benzene and 9*H*-fluorene are 5.9 × 5.5, 7.7 × 4.3 and 8.4 × 5.4 Å<sup>2</sup> as disclosed by Chem 3D software with energy minimization. Therefore, the lower efficiency of 9*H*-fluorene might be due to its bigger molecule size.

A plausible reaction mechanism for the biomimetic catalytic oxidation initiated by Cu-PMOF-3(Fe)/NHPI is proposed, which is carried out under the synergistic catalysis of metalloporphyrin and NHPI (Figure 6a, path a). Within the framework, the metalloporphyrin unit reacts with O<sub>2</sub> from the air to form the dioxygen-coordinated metalloporphyrin intermediates (**A**), which extract the hydrogen atom from NHPI to form the hydroperoxo intermediate (**B**) followed by the high-valent oxo-metal intermediate (**C**).<sup>57</sup> It is reported that O<sub>2</sub>

could be coordinated to the metal center in the porphyrin ring via an  $\eta^1$ , end-on binding mode.<sup>58,59</sup> The oxygen atom of the oxygenated metalloporphyrin (C) is then inserted into the C–H bond of ethylbenzene to realize aerobic oxidation.

Meanwhile, after the loss of the hydrogen atom, NHPI is transformed to the phthalimido-*N*-oxyl (PINO) radical, which then extracts the hydrogen atom from the benzyl C–H bond to generate an organic radical that reacts with  $O_2$  to afford the oxygenated product (Figure 6b, path b).<sup>60,61</sup> Considering that the reaction yield is 82% in the presence of both Cu-PMOF-3(Fe) and NHPI, whereas the yield is decreased to 13% when NHPI is used alone (Table 1, entries 4 and 5), path b can't explain the high efficiency of Cu-PMOF-3(Fe)-catalyzed oxidation.

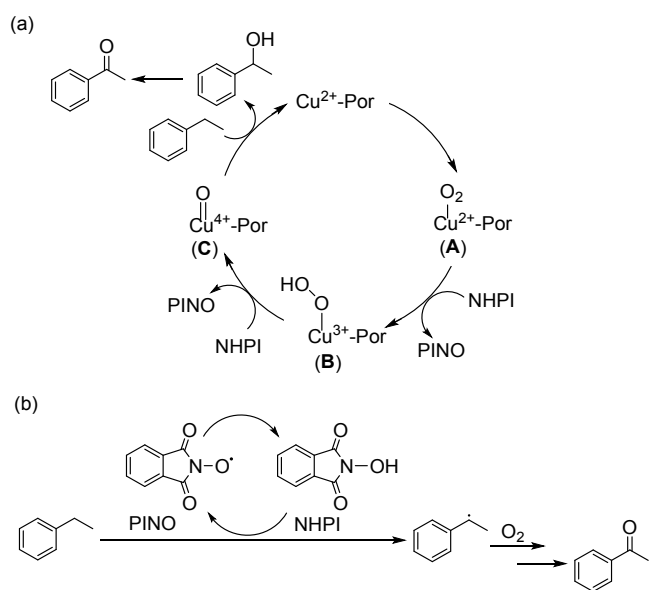


**Figure 6.** The possible mechanism of aerobic oxidation of ethylbenzene catalyzed by Cu-PMOF-3(Fe)/NHPI.

#### 4. Conclusion

In summary, an improved modulating synthesis strategy using a pair of monocarboxylic acids and water as the three-component modulator has been developed and then applied for the construction of Fe-based porphyrinic metal-organic frameworks. The prepared materials exhibit high stability, especially regarding to hydrolysis, and high catalytic performances in the aerobic oxidation of C–H bonds in the air. Further work on the design and catalytic applications of porphyrinic metal-organic frameworks is in progress.

#### Conflicts of interest

There are no conflicts to declare.

#### Acknowledgements

The authors acknowledge support from the National Natural Science Foundation of China (21773314, 21720102007,

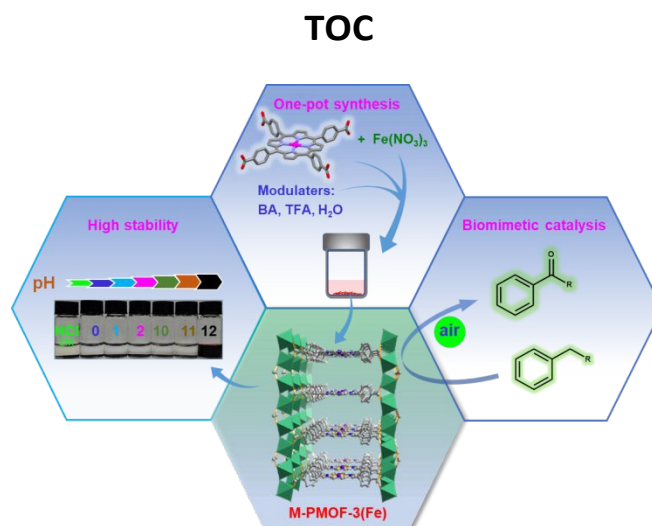
21821003, and 21890380), the Guangdong Natural Science Funds for Distinguished Young Scholar (2019B151502017), the Tip-top Youth Talents of Guangdong special support program (No. 20173100042150021), Science and Technology Planning Project of Guangzhou (201707010168), and Local Innovative and Research Teams Project of Guangdong Pearl River Talents Program (2017BT01C161).

#### Notes and references

- C.-M. Che and J.-S. Huang, *Chem. Commun.*, 2009, 3996–4015.
- H. Lu and X. P. Zhang, *Chem. Soc. Rev.*, 2011, **40**, 1899–1909.
- M. M. Pereira, L. D. Dias and M. J. F. Calvete, *ACS Catal.*, 2018, **8**, 10784–10808.
- F. Bedioui, *Coord. Chem. Rev.*, 1995, **144**, 39–68.
- P.-J. Wei, G.-Q. Yu, Y. Naruta and J.-G. Liu, *Angew. Chem. Int. Ed.*, 2014, **53**, 6659–6663.
- S. Deng, P. Yuan, X. Ji, D. Shan and X. Zhang, *ACS Appl. Mater. Interfaces* 2015, **7**, 543–552.
- K. Eriksson, E. Göthelid, C. Puglia, J.-E. Bäckvall and S. Oscarsson, *J. Catal.*, 2013, **303**, 16–21.
- W.-Y. Gao, M. Chrzanowski and S. Ma, *Chem. Soc. Rev.*, 2014, **43**, 5841–5866.
- M. Zhang, Z.-Y. Gu, M. Bosch, Z. Perry and H.-C. Zhou, *Coord. Chem. Rev.*, 2015, **293–294**, 327–356.
- Y. Chen and S. Ma, *Dalton Trans.*, 2016, **45**, 9744–9753.
- K. Chen and C.-D. Wu, *Chem. Soc. Rev.*, 2019, **378**, 445–465.
- Y. Liu and Z. Tang, *Adv. Mater.*, 2013, **25**, 5819–5825.
- M. Zhao, K. Yuan, Y. Wang, G. Li, J. Guo, L. Gu, W. Hu, H. Zhao and Z. Tang, *Nature*, 2016, **539**, 76–80.
- G. Li, S. Zhao, Y. Zhang and Z. Tang, *Adv. Mater.*, 2018, 1800702.
- D. Liu, J. Wan, G. Pang and Z. Tang, *Adv. Mater.*, 2019, **31**, 1803291.
- V. Lykourinou, Y. Chen, X.-S. Wang, L. Meng, T. Hoang, L.-J. Ming, R. L. Musselman and S. Ma, *J. Am. Chem. Soc.*, 2011, **133**, 10382–10385.
- D. Feng, Z.-Y. Gu, J.-R. Li, H.-L. Jiang, Z. Wei and H.-C. Zhou, *Angew. Chem. Int. Ed.*, 2012, **51**, 10307–10310.
- C. Zou, Z. Zhang, X. Xu, Q. Gong, J. Li and C.-D. Wu, *J. Am. Chem. Soc.*, 2012, **134**, 87–90.
- Y. Wang, H. Cui, Z.-W. Wei, H.-P. Wang, L. Zhang and C.-Y. Su, *Chem. Sci.*, 2017, **8**, 775–780.
- J. Liu, Y.-Z. Fan, X. Li, Z. Wei, Y.-W. Xu, L. Zhang and C.-Y. Su, *Appl. Catal. B*, 2018, **231**, 173–181.
- J. Liu, Y.-Z. Fan, X. Li, Z. Wei, L. Zhang and C.-Y. Su, *ChemSusChem* 2018, **11**, 2340–2347.
- S. Li, H.-M. Mei, S.-L. Yao, Z.-Y. Chen, Y.-L. Lu, L. Zhang and C.-Y. Su, *Chem. Sci.*, 2019, **10**, 10577–10585.
- M. Ding, X. Cai and H.-L. Jiang, *Chem. Sci.*, 2019, **10**, 10209–10230.
- Y. Keum, S. Park, Y.-P. Chen and J. Park, *Angew. Chem.*, 2018, **130**, 15068–15072.
- S. Yuan, T.-F. Liu, D. Feng, J. Tian, K. Wang, J. Qin, Q. Zhang, Y.-P. Chen, M. Bosch, L. Zou, S. J. Teat, S. J. Dalgarno and H.-C. Zhou, *Chem. Sci.*, 2015, **6**, 3926–3930.
- Y. Zhao, N. Kornienko, Z. Liu, C. Zhu, S. Asahina, T.-R. Kuo, W. Bao, C. Xie, A. Hexemer, O. Terasaki, P. Yang and O. M. Yaghi, *J. Am. Chem. Soc.*, 2015, **137**, 2199–2202.
- J. Zheng, M. Wu, F. Jiang, W. Su and M. Hong, *Chem. Sci.*, 2015, **6**, 3466–3470.
- Q. Lin, X. Bu, A. Kong, C. Mao, X. Zhao, F. Bu and P. Feng, *J. Am. Chem. Soc.*, 2015, **137**, 2235–2238.
- M. H. Beyzavi, N. A. Vermeulen, A. J. Howarth, S. Tussupbayev, A. B. League, N. M. Schweitzer, J. R. Gallagher,

- A. E. Platero-Prats, N. Hafezi, A. A. Sarjeant, J. T. Miller, K. W. Chapman, J. F. Stoddart, C. J. Cramer, J. T. Hupp and O. K. Farha, *J. Am. Chem. Soc.*, 2015, **137**, 13624–13631.
- 30 D. Feng, W.-C. Chung, Z. Wei, Z.-Y. Gu, H.-. Jiang, Y.-P. Chen, D. J. Darensbourg and H.-C. Zhou, *J. Am. Chem. Soc.*, 2013, **135**, 17105–17110.
- 31 A. Fateeva, P. A. Chater, C. P. Ireland, A. A. Tahir, Y. Z. Khimyak, P. V. Wiper, J. R. Darwent and M. J. Rosseinsky, *Angew. Chem. Int. Ed.*, 2012, **51**, 7440–7444.
- 32 F. Leng, H. Liu, M. Ding, Q.-P. Lin and H.-L. Jiang, *ACS Catal.*, 2018, **8**, 4583–4590.
- 33 K. Wang, D. Feng, T.-F. Liu, J. Su, S. Yuan, Y.-P. Chen, M. Bosch, X. Zou and H.-C. Zhou, *J. Am. Chem. Soc.*, 2014, **136**, 13983–13986.
- 34 X.-L. Lv, K. Wang, B. Wang, J. Su, X. Zou, Y. Xie, J.-R. Li and H.-C. Zhou, *J. Am. Chem. Soc.*, 2017, **139**, 211–217.
- 35 E.-X. Chen, M. Qiu, Y.-F. Zhang, Y.-S. Zhu, L.-Y. Liu, Y.-Y. Sun, X. Bu, J. Zhang and Q. Lin, *Adv. Mater.*, 2018, **30**, 1704388.
- 36 A. Fateeva, J. Clarisse, G. Pilet, J.-M. Grenèche, F. Nouar, B. K. Abeykoon, F. Guegan, C. Goutaudier, D. Luneau, J. E. Warren, M. J. Rosseinsky and T. Devic, *Cryst. Growth Des.*, 2015, **15**, 1819–1826.
- 37 A. Fateeva, S. Devautour-Vinot, N. Heymans, T. Devic, J.-M. Grenèche, S. Wuttke, S. Miller, A. Lago, C. Serre, G. De Weireld, G. Maurin, A. Vimont and G. Férey, *Chem. Mater.*, 2011, **23**, 4641–4651.
- 38 M. Bosch, S. Yuan, W. Rutledge and H.-C. Zhou, *Acc. Chem. Res.*, 2017, **50**, 857–865.
- 39 T. He, B. Ni, X. Xu, H. Li, H. Lin, W. Yuan, J. Luo, W. Hu and X. Wang, *ACS Appl. Mater. Interfaces* 2017, **9**, 22732–22738.
- 40 T. Tsuruoka, S. Furukawa, Y. Takashima, K. Yoshida, S. Isoda and S. Kitagawa, *Angew. Chem. Int. Ed.*, 2009, **48**, 4739–4743.
- 41 A. Schaate, P. Roy, A. Godt, J. Lippke, F. Waltz, M. Wiebcke and P. Behrens, *Chem. Eur. J.*, 2011, **17**, 6643–6651.
- 42 T. He, X. Xu, B. Ni, H. Wang, Y. Long, W. Hu and X. Wang, *Nanoscale*, 2017, **9**, 19209–19215.
- 43 Z. Hu, I. Castano, S. Wang, Y. Wang, Y. Peng, Y. Qian, C. Chi, X. Wang and D. Zhao, *Cryst. Growth Des.*, 2016, **16**, 2295 – 2301.
- 44 Z. Hu, A. Nalaparaju, Y. Peng, J. Jiang and D. Zhao, *Inorg. Chem.*, 2016, **55**, 1134–1141.
- 45 G. C. Shearer, S. Chavan, S. Bordiga, S. Svelle, U. Olsbye and K. P. Lillerud, *Chem. Mater.*, 2016, **28**, 3749–3761.
- 46 G. C. Shearer, S. Chavan, J. Ethiraj, J. G. Vitillo, S. Svelle, U. Olsbye, C. Lamberti, S. Bordiga and K. P. Lillerud, *Chem. Mater.*, 2014, **26**, 4068–4071.
- 47 F. Vermoortele, B. Bueken, G. Le Bars, B. Van de Voorde, M. Vandichel, K. Houthoofd, A. Vimont, M. Daturi, M. Waroquier, V. Van Speybroeck, C. Kirschhock and D. E. De Vos, *J. Am. Chem. Soc.*, 2013, **135**, 11465–11468.
- 48 P. L. Llewellyn, P. Horcajada, G. Maurin, T. Devic, N. Rosenbach, S. Bourrelly, C. Serre, D. Vincent, S. Loera-Serna, Y. Filinchuk, and G. Férey, *J. Am. Chem. Soc.*, 2009, **131**, 13002–13008.
- 49 A. Fateeva, P. Horcajada, T. Devic, C. Serre, J. Marrot, J.-M. Grenèche, M. Morcrette, J.-M. Tarascon, G. Maurin and G. Férey, *Eur. J. Inorg. Chem.*, 2010, 3789–3794.
- 50 H. Jia, Z. Sun, D. Jiang, S. Yang and P. Du, *Inorg. Chem. Front.*, 2016, **3**, 821–827.
- 51 J. M. Gottfried, K. Flechtner, A. Kretschmann, T. Lukaszczuk and H.-P. Steinrück, *J. Am. Chem. Soc.*, 2006, **128**, 5644–5645.
- 52 W. Zhang, W. Gao, T. Pham, P. Jiang and S. Ma, *Cryst. Growth Des.*, 2016, **16**, 1005–1009.
- 53 W. Zhao, W. Wang, J. Peng, T. Chen, B. Jin, S. Liu, W. Huang and Q. Zhao, *Dalton Trans.*, 2019, **48**, 9631–9638.
- 54 S. Shaik, S. Cohen, Y. Wang, H. Chen, D. Kumar and W. Thiel, *Chem. Rev.*, 2010, **110**, 949–1017.
- 55 L. J. J. Laarhoven and P. Mulder, *J. Phys. Chem. B*, 1997, **101**, 73–77.
- 56 S. E. Stein and R. L. Brown, *J. Am. Chem. Soc.*, 1991, **113**, 787–793.
- 57 M. Zhao and C.-D. Wu, *ChemCatChem*, 2017, **9**, 1192–1196.
- 58 A. T. Gallagher, M. L. Kelty, J. G. Park, J. S. Anderson, J. A. Mason, J. P. S. Walsh, S. L. Collins and T. D. Harris, *Inorg. Chem. Front.*, 2016, **3**, 536–540.
- 59 J. S. Anderson, A. T. Gallagher, J. A. Mason and T. D. Harris, *J. Am. Chem. Soc.*, 2014, **136**, 16489–16492.
- 60 D. P. Hruszkewycz, K. C. Miles, O. R. Thiel and S. S. Stahl, *Chem. Sci.*, 2017, **8**, 1282–1287.
- 61 Z. Tan, J. Zhu and W. Yang, *Catal. Commun.*, 2017, **94**, 60–64.

## ARTICLE



A facile synthesis of a series of Fe-oxo chain-based porphyrinic MOFs (namely M-PMOF-3(Fe), M = Fe, Co, Ni, Cu) has been reported.